RESEARCH ARTICLE

I2MB: Intelligent Immersive Multimedia Broadcast in Next-Generation Cellular Networks

CHETNA SINGHAL, (Senior Member, IEEE)
Department of Electronics and Electrical Communication Engineering, Indian Institute of Technology Kharagpur, Kharagpur, West Bengal 721302, India
Department of Computer Science, RISE Research Institutes of Sweden AB, 16440 Stockholm, Sweden

e-mail: chetna.iitd@gmail.com

ABSTRACT The popularity of immersive multimedia content is prevalent and the consumption of 360° videos is increasing rapidly in varied domains. The broadcast of such content in cellular networks will be challenging in terms of dynamic content adaptation and efficient resource allocation to serve heterogeneous consumers. In this work, we propose an intelligent immersive new radio multimedia broadcast multicast system (NR-MBMS), I2MB, for next-generation cellular networks. I2MB intelligently forecasts the users' viewing angle and the 360° video tiles to be broadcast beforehand using long short-term memory network. We define broadcast areas by using modified K-means clustering. The complex multivariable optimization problem that integrates efficient adaptive 360-degree video encoding and tiled broadcast using optimized transmission parameters is defined as as a Markov decision process (MDP). In a dense urban scenario with a large MBSFN (multimedia broadcast multicast service single frequency network) synchronization area, the state and action space dimensionality is very high, in which the solution is obtained by using deep deterministic policy gradient (DDPG) algorithm. I2MB incorporates deep reinforcement learning based radio resource allocation (modulation-coding scheme and frequency-time resource blocks) and tiled video encoding to maximize the viewport video quality experienced by the broadcast mobile users. I2MB provides improved immersive video broadcast streaming quality while serving a higher number of mobile users. Adaptive encoding of 360° video tiles and radio resource allocation are performed based on users' forecasted viewing angle, spatial distribution, channel conditions, and service request. The performance evaluation of our proposed scheme, I2MB, shows considerable gains in viewport quality (46.83%) and number of users served (30.52%), over a recent state-of-the-art method VRCAST.

INDEX TERMS Multimedia broadcast and multicast services (MBMS), new radio MBMS (NR-MBMS), 360° video, viewing angle prediction, immersive tiled video.

I. INTRODUCTION

Immersive 360° video streaming is increasingly used in diverse applications such as virtual reality, gaming, and entertainment [1]. In the immersive environment, when a viewer changes their viewing direction, the content is accordingly rendered. However, streaming such content requires very high bandwidth and is challenging [1]. A 360° immersive video can be divided into small portions spatially known as 'tiles' that can be encoded at different quality levels.

The associate editor coordinating the review of this manuscript and approving it for publication was Jon Montalban.

This has enabled tiling-based viewport-adaptive 360° video streaming, where tiles are delivered to clients based on their viewing direction and network conditions. Concretely, the tiles within the user's viewport can be transmitted at a higher quality, while the rest of the tiles can be delivered at a lower quality [2].

Digital television (TV) broadcast is a popular service in wireless networks comprising on-demand content streaming and multimedia broadcast to heterogeneous customers on their smart devices like TVs, phones, and car-infotainment systems [3]. Streaming on-demand multimedia data to mobile users using unicast transmission requires considerably higher

amounts of network resources and it is difficult to scale up to a urban dense network scenario. Multicast/broadcast instead offer a more scalable solution, but face certain difficulties like, user-centric adaptation, responsiveness to user interactivity, and providing seamless quality. This motivates the investigation of resource efficient 360° video broadcast solutions for future large/dense cellular networks.

The further evolved multimedia broadcast multicast services (FeMBMS) standard, defined in 3GPP Release 14, provides for multimedia streaming over cellular network [4]. With the advent of next generation communication standards, efforts are being made to define NR-MBMS (5G New Radio MBMS) and advance FeMBMS [5]. Herein, *synchronization area*, is an important definition, within which the associated 3GPP 5G Next Generation base stations (gNBs) need to be time synchronized. According to the standard, the multimedia broadcast multicast service single frequency network (MBSFN) consists of a group of gNBs that broadcast the same content using the same set of radio resources, simultaneously, within a synchronization area. Thereby, at the receiver a better quality can be ensured by combining the signal received from various gNBs. The broadcast along with the unicast transmission can be simultaneously facilitated within each cell of an MBSFN area, and cell capacity can be shared for both.
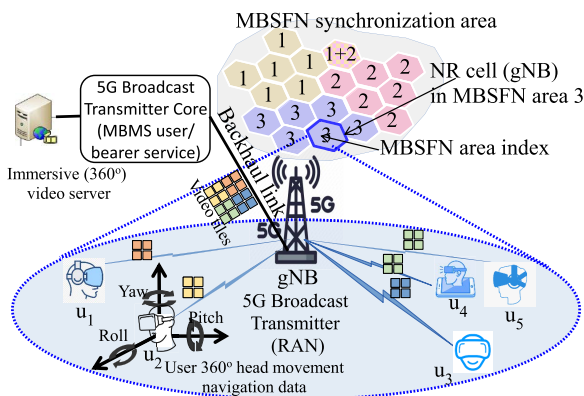

FIGURE 1. I2MB Scenario in 5G NR networks.

We have developed an intelligent immersive (360°) multimedia broadcast solution, I2MB, that can be deployed in future cellular networks and is suitable for large and dense network scenarios. Fig. 1 shows a sample scenario of I2MB in 5G-NR cellular networks. The heterogeneous users will have diverse user equipment, program requests, viewing directions, and gNodeB (gNB) association. The broadcast transmitter (gNB) in the radio access network fetches the broadcast content from the video server through the broadcast transmitter core element and broadcasts the tiles subject to viewport of associated users. The tiles of an immersive video are sent from the multimedia server to gNB using the backhaul link. The MBMS user and bearer services are managed by the broadcast transmitter element in the core that also maintains the MBSFN area formation and resource allocation. Each

MBSFN comprises of several gNBs that broadcast same set of programs in a synchronized manner using the same set of radio resources. A gNB can be a part of more than one MBSFN area. In the given example, a cell is shown to be a member of two MBSFN areas: $\{1, 2\}$. The users $u_1 - u_6$ are accessing the 360° multimedia program at different viewing angles and are receiving the corresponding tiles in their viewport.

The trend in viewing and popularity of TV content (i.e. programs and TV channels) is found to be dependent on demography, social, economical, age, and region specific factors of the viewers [6], [7], [8]. Ratings of TV channels, programs, and audience can help in deciding content production and schedules [9]. Multiple channel TV service has another alternative over-the-top (OTT) streaming that has behavioral advertising based monetization [10]. Overall, it motivates us to group users using multi-criteria clustering to form MBSFN areas. We perform NR-MBMS resource allocation based on multiple parameters: user content interest (request), viewing direction angles, gNB association, and program popularity, in a given MBSFN synchronization area. In our proposed scheme, I2MB, we form MBSFN area by grouping cells while considering user content request, location, experienced channel conditions, and user head navigation direction.

Given a set of MBSFNs, we aim to maximize the immersive quality delivered to the users by adaptively encoding 360° video tile and efficiently allocating radio resource. We have formulated an algorithm based on deep reinforcement learning (DRL) that executes at the broadcast transmitter (BTx) to efficiently allocate radio resources and adaptively encode the 360° video tiles that have to be broadcast. The aim is to minimize the sum-distortion and churn rate experienced by the users in the system. The users' program requests, viewing directions, and channel conditions are considered to be unknown to the users and the BTx beforehand. We demonstrate using performance evaluation results considerable gains in viewport peak signal to noise ratio (PSNR) and number of served users, over a recent state-of-the-art method VRCAST.

The rest of the paper is organized as follows. Section II discusses related works. Section III presents the I2MB system architecture and components. Section IV describes the I2MB framework consisting of User head navigation direction forecasting, MBSFN formation using multi-criteria clustering, and deep reinforcement learning based tile quality adaptation and resource allocation. Section V provides details on the simulation scenario and presents the key performance results. Finally, Section VI draws our conclusions.

II. RELATED WORK AND KEY CONTRIBUTIONS
Adaptive 360° video streaming based on users' viewport has been studied in [1] and [2] via the design of efficient 360° video representations and resource allocation methods. Live scalable 360° video network multicast has been investigated in [11] via rate-distortion optimization and user viewport prediction. The reference method we consider in our

experiments is known as VRCAST and has been studied in [12] for streaming of live 360° videos to mobile users. It considers grouping of users, adaptive resource allocation, and tile-quality selection. However, it focuses on live multicast and does not address multiple parallel broadcast sessions for larger and denser cellular networks, where a unilateral channel condition based grouping for a limited number of users fails. Our approach aims to fill this gap.

LTE eMBMS resource allocation for multimedia streaming to heterogeneous users with diverse channel conditions is discussed in [13]. However, adaptive encoding of immersive multimedia content, user heterogeneity, and quality assurance are also important factors that need due consideration. Similarly, multicast transmission can be optimized by dynamically defining the MBSFN areas and has been discussed in [14]. However, multi-criteria heterogeneous user clustering to efficiently define MBSFN areas, efficient encoding of 360° immersive multimedia tiles, and NR-MBMS resource allocation optimization, as considered in this paper, represents a novel topic that has not been studied before.

Time series forecasting using long short-term memory (LSTM) deep learning model has been used for C-reactive protein used in cancer immunotherapy clinical decision making [15]. LSTM deep learning model with with adaptive moment estimation (Adam) has been used for multi-step ahead time series prediction [16]. Deep learning LSTM model has been used to forecast short-term electricity supply load [17]. Traffic demand forecasts is essential for transportation network companies to properly allocate resources and avoid delays in services provisioning. This involves long-, medium, and short-term forecasting that can be implemented using deep neural networks [18]. The cellular metrics (connections, throughput) can be forecast in social events using LSTM deep learning model that is applied to the social information and data from past events [19].

Reinforcement learning has self-learning ability and good generality [20]. The channel dynamics and user requests are governed by the stochastic processes that are unknown a priori in the real-world networks. In such scenarios where system dynamics are unknown, reinforcement learning (RL) method such as Q-learning can be used [21]. Q-learning based content caching algorithm can assist the network to efficiently utilize the resource of the BSs [22]. Deep RL (DRL) can be used to optimize the wireless network operation. Deep deterministic policy gradient (DDPG) algorithm combines the architectures of deep Q-learning, deterministic policy gradient and Actor-Critic. It is suitable for continuous action space. DDPG can automate wireless network optimization [21]. It can also be used for optimal path planning of mobile robots [20]. Live streaming services for vehicular infotainment systems in the Internet of Vehicles (IoV) requires high quality, low latency, and low bitrate variance. Due to the dynamic properties of wireless channels, the live video transcoding and streaming scheme in vehicular fog-computing (VFC)-enabled IoV is achieved by using a soft actor-critic DRL DDPG algorithm [23].

The following are a few key contributions of this work:
- User head navigation direction prediction using deep learning LSTM model.
- Efficient Multi-criteria clustering based MBSFN area formation with optimal number of clusters.
- The DDPG algorithm based optimal radio resource allocation and adaptive 360° tiles encoding that minimizes the users' sum-distortion and system churn rate.
- Extensive simulation based evaluation shows the effectiveness of the proposed I2MB technique that outperforms state-of-the-art VRCAST algorithm in terms of churn rate and video quality.

III. I2MB SYSTEM ARCHITECTURE AND COMPONENTS

The architecture of our proposed I2MB system is illustrated in Figure 2. Heterogeneous user equipments (UEs) send the head navigation information to their serving gNB (RAN broadcast Transmitter). This is then used to refine the LSTM users' viewport forecast. The gNB forward this information to the broadcast transmitter core element consisting of multicast (multi-cell) coordination entity (MCE) and NR-MBMS gateway. These elements define the MBSFN area (based on multi-criteria clustering) in order to efficiently broadcast 360° immersive digital TV content to heterogeneous UEs. Thereafter, these also adaptively allocate radio resources (resource blocks, modulation and coding scheme). The content server adaptively encodes 360° video tiles using quantization level selection based on user requests, viewport (based on head movement navigation data), rate-distortion (R-D) characteristics of the immersive media content, and radio resource constraints.
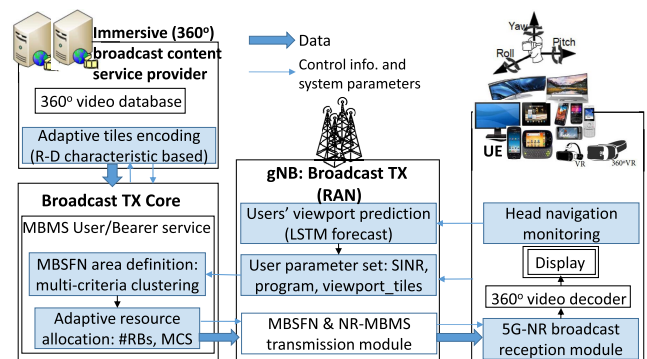
FIGURE 2. I2MB system architecture.

A. USER HEAD MOVEMENT NAVIGATION DATA AND TILE MAPPING

The user head-movement data corresponding to user navigation of a 360° video over time is monitored by the UE. At the UE, the immersive extended/ virtual reality (XR/VR) device records the viewpoint direction, V_i, of the user i, on the 360° viewing sphere. The user is considered to be positioned at the center of this sphere. This is shown in Fig. 3(b). In particular, the spherical coordinates azimuth and polar angles,
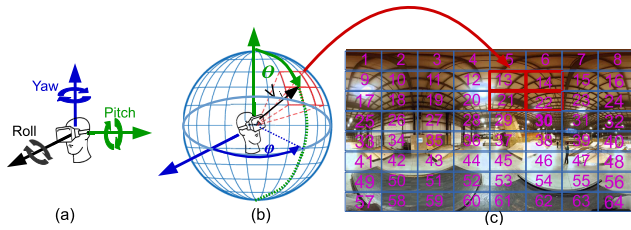
FIGURE 3. User head movement navigation: (a) Rotation angles (yaw, pitch, and roll) in three coordinate axis (b) Azimuthal and polar angles (ϕ, θ) in spherical coordinates (c) mapping to panoramic area with 8×8 spatial tiling.

$\phi \in [0^o, 360^o]$ and $\theta \in [0^o, 360^o]$ describe the surface that is normal of V_i on the 360° sphere, as shown in Fig. 3(b). These two angles are correspondingly referred to as yaw and pitch and are the rotation angles around the axes, as shown in Fig. 3(a).

The 360° video is partitioned into a set of 8×8 spatial tiles, as shown in Fig. 3(c). The tiles can be separately encoded and streamed to the user. Tiling the video at the HEVC (high efficiency video coding) encoder is possible using its tiling feature. Each tile is indexed in a raster fashion, top-to-bottom and left-to-right. The surface corresponding to viewport V_i on the sphere (c.f. Fig. 3(b)) can be mapped to the spatial tiles in the panoramic visualization of the 360° video as shown in Fig. 3(c).

B. NR-MBMS RESOURCE ALLOCATION

The channel quality indicator (CQI) is a measure of channel quality being experienced by a user. The gNB selects suitable modulation and coding scheme (MCS) to broadcast tiles to users based on CQI. In 5G-NR, grouping of radio resources into resource blocks (RBs) is used in downlink communication. Each RB consists of 12 consecutive subcarriers in frequency domain and depending on the bandwidth each lasts for 0.0625-1 ms. In practice, the resource allocation can be performed periodically every subframe. According to NR-MBMS, all subframes, i.e., 100% of the available radio resources, can be allocated for broadcasting services [4], [5]. In broadcasting, the UE experiencing the worst CQI in the group (receiving the broadcast content in an MBSFN area) governs the radio resource allocation parameters. Therefore, in order to broadcast tile τ of 360° program p using a fraction $(\sigma_\tau^p, 0 \le \sigma_\tau^p \le 1)$ of total subframes, with channel bandwidth B MHz, and allocation of MCS m_τ^p with spectral efficiency $e_{m_\tau^p}$, the capacity is given by $C(\sigma_\tau^p, m_\tau^p) = B \cdot \sigma_\tau^p \cdot e_{m_\tau^p}$. Hence, the MBSFN area capacity depends on the allocated MCS and the fraction of total subframes that are used to broadcast the 360° video tiles.

IV. I2MB: MBSFN FORMATION, TILE QUALITY ADAPTATION, AND RESOURCE ALLOCATION

We discuss our proposed framework, I2MB, that consists of MBSFN formation (Sec. IV-B) (based on user viewport forecasting and efficient clustering) and adaptive immersive tile-based multimedia encoding with corresponding network resource allocation (Sec. IV-C) to broadcast a set of immersive content to heterogeneous users in large-dense next-generation cellular networks.

A. USER HEAD NAVIGATION FORECASTING AND TILE MAPPING

We perform user head navigation direction (rotation angle) time series forecasting using LSTM regression network, a deep learning technique, with the LSTM layer specified to have > 150 hidden units. The pattern of head navigation of a user helps in forecasting the viewing direction in the immediate future (for the next GOP transmission). We train a time-series forecasting LSTM model to predict the future time step values of user viewport. We train the sequence-to-sequence regression LSTM network, where the responses are the training sequence of values that are shifted by a few time step. This means that in each time step of the input sequence, the LSTM network learns to predict the next few set of values in subsequent time steps. We forecast the values of multiple time steps in the future and predict time steps one at a time and update the network state at each prediction. We train an LSTM network to forecast the head navigation direction (rotation angle) of each user given the previous time-step direction information. The predictor is trained by ADAM optimizer [24], [25] for the non-stationary head navigation data of immersive multimedia users.

Since, the monitored head navigation information is sent to the broadcast transmitter (gNB), the actual values of time steps are accessible between predictions. Hence, the observed values are used to update the network state instead of the predicted values. We begin by initializing the network state and proceed thereafter by resetting it to prevent previous predictions from affecting the predictions in subsequent time steps. For each prediction in each time step, prediction in subsequent time step uses the observed value (at the users' head navigation monitoring module) of the previous time step. The prediction accuracy is enhanced when the network state is updated with the observed values instead of the predicted values [16]. The prediction model performance is evaluated using root mean squared error (RMSE), defined as:

$$RMSE = \sqrt{\frac{1}{\nu} \sum_{i=1}^{\nu} (\mathcal{A}_i - \mathcal{F}_i)^2}, \qquad (1)$$

where, $\mathcal{A}_i$ is the actual value and $\mathcal{F}_i$ is the predicted value during forecasting and ν is the total number of time steps over which the prediction has been performed.

B. MBSFN AREA FORMATION: MULTI-CRITERIA CLUSTERING

The heterogeneous users within the MBSFN synchronization area have diverse program requests, gNB association, and user location. The heterogeneous users report their CQI, head navigation direction (i.e. viewing angle), and the requested 360° video program to their gNB. Based on this information, the broadcast core transmitter core MCE element forms

the MBSFN areas and assigns the programs to be broadcast in each area. We perform multi-criteria clustering based on information pertaining to each user $i \in [1, N]$, requesting for program p_i, associated with BS with position ϑ_i, and is experiencing Signal to Interference-Noise Ratio (SINR) to the the associated BS as γ_i. The clusters group UEs with similar video program requests and nearby locations. MBSFN areas are thereafter defined as group of gNBs to which user clusters are mapped. This ensures the MBSFNs suitably adapt to heterogeneous requests and distribution of UEs in a broadcast service area. We assign a set of programs, $\mathcal{P}_k \subseteq \mathcal{P}$, to be broadcast in each MBSFN k based on user requests in the corresponding cluster, the availability of radio resources, and quantization parameter selection for video-tiles.

Multi-dimensional clustering is an NP hard problem [26]. K-Means, K-medoid, and Fuzzy C-means are well known and a popular algorithms for multi-criteria clustering. We have analyzed these clustering methods to perform the MBSFN area formation. These multi-criteria clustering methods can be validated using indices like the global silhouette index, and Dunn index [27]. The distance metric for user i to the centroid c_k of a cluster k is defined as:

$$d^2(u_i, c_k) = (\vartheta_i - \vartheta_{c_k})^2 + (\gamma_i - \gamma_{c_k})^2 + \pi^2_{i,c_k},$$

$$\pi_{i,c_j} = \begin{cases} 1, & p_i \in \mathcal{P}_k \\ 0, & \text{otherwise} \end{cases}. \quad (2)$$

We evaluate the efficacy of the multi-criteria clustering methods in our cellular 360° multimedia broadcast framework using the following metrics:

1) Euclidean distance (D_e):

$$\mathcal{D}_e = \sqrt{\sum_{\forall k} d_e(k)},$$

$$d_e(k) = \frac{1}{N_k} \sum_{\forall i \in k} d^2(u_i, c_k). \quad (3)$$

User i belongs to cluster k. There are total of N_k users in cluster k. We can find the nearest neighbors using D_e.

2) Mahalanobis distance (D_m):

$$\mathcal{D}_m = X^T \cdot C^{-1} \cdot X, \quad (4)$$

$$X = \begin{bmatrix} \sqrt{d_e(1)} \\ \vdots \\ \sqrt{d_e(k)} \\ \vdots \\ \sqrt{d_e(K)} \end{bmatrix},$$

C matrix contains covariance withing each cluster as the diagonal elements. D_m accounts for correlatedness between the clustering variables. While considering covariance between the cluster points redundancy is removed in the distance calculation.

3) Silhouette coefficient ($\mathcal{S}$): This measure validates consistency in clusters and similarity of an object with its cluster

(cohesion) compared to other clusters (separation). It is used to evaluate the distance of separation between the clusters resulting from the used method [28]. The silhouette plot visually shows closeness of points in a cluster than to those in neighboring clusters.

$$\mathcal{S} = \frac{1}{K} \sum_{k=1}^{K} S_k,$$

$$S_k = \frac{1}{N_k} \sum_{i=1}^{N_k} s_i, \quad s_i = \frac{b_i - a_i}{\max(a_i, b_i)}, \quad (5)$$

where, s_i ($-1 \leq s_i \leq 1$) is the Silhoutte width, a confidence indicator on the membership of i in cluster k. When s_i is close to 1, it indicates that i is well clustered (i.e., assigned to appropriate cluster). When s_i is close to zero, indicates that i can also be assigned to the closest neighboring cluster [27]. The average distance between i and all other users included in k is denoted as a_i and minimum of the average distance between i and all of the samples clustered in k' ($k \neq k', 1 \leq k \leq K$) is denoted as b_i.

The partition that results in the maximum value of $\mathcal{S}$ is the optimal corresponding to the most appropriate number of Clusters, i.e. optimal K [29].

4) Dunn's index (DI): This validity index aims to identify clusters with a high inter-cluster and low intra-cluster distance.

$$DI = \min_{1 \leq k \leq K} \left\{ \min_{1 \leq k' \leq K, k \neq k'} \left\{ \frac{d(c_k, c_{k'})}{\max\limits_{1 \leq k \leq K} \{\Delta c_k\}} \right\} \right\},$$

$$\Delta(c_k) = \max_{i,j \in k} \{d(i, j)\}. \quad (6)$$

$\Delta(c_k)$ represents the complete diameter intracluster distance of cluster k. This measure maximizes the intercluster while minimizing intracluster distances. A large value of DI corresponds to good clusters [27]. The number of clusters that maximizes DI could be taken as the optimal number of clusters and a higher value represents a better cluster quality.

The Dunn [30] and Silhouette [28] coefficient result from nonlinear combination of compactness and separation.

We begin by setting K, i.e. number of clusters, as 1. Thereafter in each iteration, we increase K by 1. When the performance metric obtained is better that the previous iteration, the algorithm continues till a drop in performance is observed. This gives us the optimal size of cluster, K^*. According to the 3GPP standard, a gNB can belong to at most 8 MBSFN areas, we ensure that this limitation is enforced i.e. a gNB can be associated with maximum 8 clusters at a time. These clusters would have the highest proportion of UEs associated with the gNB. The proposed I2MB MBSFN area formation multi-criteria clustering framework is given in Algorithm 1, Function I. This function in the algorithm gives the K MBSFN areas, the set of 360° programs to be broadcast in K (i.e. $\mathcal{P}_k$), and the video tiles to be broadcast.

C. DEEP REINFORCEMENT LEARNING BASED ADAPTIVE IMMERSIVE TILE ENCODING AND RESOURCE ALLOCATION
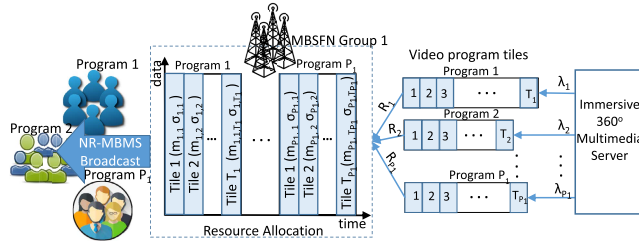

FIGURE 4. I2MB: DRL system model.

Multicriteria clustering gives us a set of MBSFN areas with the list of associated gNB and users as well as the set of 360° video programs and tiles to be broadcast. We model the logical resource allocation (MCS, $m_{p,\tau}^k$, and proportion of SFs, $\sigma_{p,\tau}^k$) and efficient tile encoding using the MDP shown in Fig. 4. The immersive video tiles ($1 \leq \tau \leq T_p$) of the 360° TV programs ($1 \leq p \leq P_k$) are being broadcast in MBSFN area k ($1 \leq k \leq K$).

The broadcasting decisions include the following: (i) program and tile set to be broadcast given the radio resource constraints, (ii) quantization level selection for tiles encoding of the 360° TV program, and (iii) resource block proportion and MCS level to broadcasting the required tiles of each program in the set. The radio resource (i.e. broadcast spectrum) is distributed between the 360° broadcast content tiles, each being transmitted in a time interval (TTI), i.e. the smallest time unit that can be allocated. The resource allocation module is deployed in BTx that coordinates with the gNBs (in MBSFN areas) and the granularity scale is one subframe and a RB in the time-frequency domain, respectively. The allocation of radio resources to tiled broadcast happens in every decision interval, where the proportion of RBs allocated to a particular program p and tile τ is indicated by the metric $\sigma_{p,\tau}$.

The gNB allocates resources to a tile of program being broadcast in every TTI. Our intelligent immersive tile-based multimedia encoding and radio resource allocation scheme minimizes the users' 360° video distortion and system churn rate, accounting for different UE requests, viewing angles, and channel conditions. Corresponding to the MBSFN area 1, as shown in Fig. 4, the video tiles data of programs $p \in [1, P_1]$ are arriving at the broadcast transmitter (group of gNBS) from the immersive 360° video server at a rate λ_p.
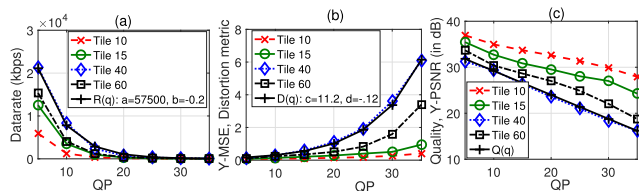

FIGURE 5. (a) Rate, (b) Y-MSE, and (b) Quality, with analytical model and variation with QP level for a 360-degree video.

In the following discussions, we consider that each UE at any given point of time is requesting at most 1 360° program. We denotes the maximum number of tiles of a 360° program p as T_p. We define the 360° immersive multimedia broadcast service distortion for heterogeneous UEs as follows:

Definition 1: Immersive video distortion is governed by the rate-distortion (R-D) characteristics of the video. The video bitrate varies with the variation of quantization parameter (QP) at the encoder. In particular, QP is a video encoding parameter that regulates the extent of spatial detail in encoded video. As QP is increased, the bit rate drops in exchange for increased distortion. It is related to quantization step size q as: $q = 2^{(QP-4)/6}$. Effectively, the user i viewport distortion is given as:

$$\mathcal{D}_i = \sum_{\forall \tau,\, 1 \leq \tau \leq T_p} \alpha_{\tau,i} D_\tau(R_\tau),$$

$$\alpha_{\tau,i} = \begin{cases} 1, & \text{if } \tau \text{ is in viewport } V_i \\ 0, & \text{otherwise.} \end{cases} \quad (7)$$

$\alpha_{\tau,i}$ *is an indicator of tile τ appearing in user i's viewport V_i for the requested program p.*

Correspondingly, the video quality, Y-PSNR, is given as: $Q_i = 10 \cdot \log_{10}(I_{max}/D_i)$, I_{max} *is the peak luminance intensity, given that D_i is the luminance mean square error (Y-MSE).* We define system (network) churn rate for I2MB as follows.

Definition 1: System (network) churn rate is the ratio of the unserved and the total users in the system. A user i is served if it successfully receives the tiles in its viewport V_i and is given as:

$$Cr = \frac{\sum_{i=1}^{N}(1 - \beta_{\tau,i})}{N},$$

$$\beta\tau, i = \begin{cases} 1, & \text{if } \gamma_i \geq SINR\_thr(m_{\tau_i}^p),\, Q(q_{p,\tau_i}) \geq Q_{min}, \\ & \text{and } \alpha_{\tau,i} = 1 \\ 0, & \text{otherwise.} \end{cases} \quad (8)$$

SINR_thr denotes the SINR threshold corresponding to the MCS m_{p,τ_i}^k selected for transmission of corresponding tile. $\beta_{\tau,i}$ is an indicator of tile τ being successfully received by user i. The condition $Q(q_{p,\tau_i}) \geq Q_{min}$ and $\gamma_i \geq SINR\_thr(m_{\tau_i}^p)$ ensures that the served user gets an acceptable minimum quality level. A lower value of churn rate is desired in the system, which would signify an increased number of users are getting serviced in the network.

We assume that channel characteristics remain stationary, i.e. SINR experienced by users remains constant, during the broadcast of all tiles (T_p) for a group of picture (GOP) of the requested 360° program. We also assume that the number of users in the system remains constant for the time duration of GOP broadcast of the requested program. Therefore, a UE can successfully receive immersive video tile τ_i (in its viewport) if its experienced SINR is greater than the threshold corresponding to the MCS m_{p,τ_i}^k that is being used to broadcast tile τ_i of p in MBSFN k. Only when the 360° multimedia service quality experienced by user i is above

minimum acceptable level corresponding to rate supported by the MCS allocated for its transmission, i.e. m_{p,τ_i}^k, we consider the corresponding quality. It is assumed to be zero other wise.

The SINR pertaining to the worst channel condition user amongst those requesting tile τ of program p at time t is denoted as $\gamma_{p,\tau}^t$. The corresponding set containing the SINR value for all tiles of program p is $\boldsymbol{\gamma}_p^t = \{\gamma_{p,1}, \ldots, \gamma_{p,T_p}^t\}$. The combined state of all 360° programs and their tiles is given by the matrix $\boldsymbol{\Gamma}^t$.

The 360° program p's stream status at time t is represented by $\mathcal{R}_p^t$. The combined state of all 360° program streams at time t is given by the vector $\boldsymbol{\mathcal{R}}^t = \{\mathcal{R}_1 \ldots \mathcal{R}_{\mathcal{P}_k}\}$. We assume that new set of data is arriving from the immersive 360° multimedia server with independent and identical distribution (i.i.d.). The average arrival rate of the p-th program data is denoted by λ_p (bits/s). The program data (i.e. tiles) arriving in time slot t is denoted by l_p^t. The 360° program p's stream state in the next time slot, i.e. $t + 1$, is given by the following Lindley recursion,

$$\mathcal{R}_p^{t+1} = \max(0, \mathcal{R}_p^t - a_p^t(\boldsymbol{\mathcal{R}}^t, \boldsymbol{\Gamma}^t)) + l_p^t, \qquad (9)$$

where, $a_p^t(\boldsymbol{\mathcal{R}}^t, \boldsymbol{\Gamma}^t)$ denotes the amount of data of program p for transmission based on resource allocation action. Given the arrival distribution P_p^l and the resource allocation action a_p, the probability that program p stream transitions from state $\mathcal{R}_p$ to $\mathcal{R}_p'$ is,

$$P_p^{\mathcal{R}}(\mathcal{R}_p'|\mathcal{R}_p, a_p) = \mathbb{E}_l[\mathbb{I}_{\{\mathcal{R}_p'=\max(0, \mathcal{R}_p^t - a_p^t(\boldsymbol{\mathcal{R}}^t, \boldsymbol{\Gamma}^t))+l_p^t\}}], (10)$$

where $\mathbb{I}_{\{\cdot\}}$ is an indicator function that takes a value 1 when $\{\cdot\}$ is true, and 0 otherwise. The state of a program p stream to be broadcast in an MBSFN area k is defined as $s_p \triangleq (\mathcal{R}_p, \boldsymbol{\gamma}_p)$ and the system state is $s = \{s_1 \ldots s_{\mathcal{P}_k}\}$.

The mapping of states to resource allocation actions is a *policy* that is denoted as $\Pi : \mathcal{S} \to A$. The objective is to minimize the average sum of 360° program distortion experienced by users and the system churn rate by selecting the optimal (best) policy Π^* and thereby performing the resource allocation and efficient encoding. Since the resource allocation decisions at the current time affect the present and the future distortion-churn rate experienced by the UEs, we formulate the broadcast resource and encoding parameter allocation problem as MDP.

We define a program stream cost that applies penalty to higher distortion and churn rate in the system. Given stream state s_p^t and the resource allocation action a_p^t, we program p's stream cost in time slot t as the change in state from time t to $t + 1$ is defined as:

$$c_p^t(s_p^t, a_p^t) = [\max(0, \mathcal{R}_p^t - a_p^t) + l_p^t] - \mathcal{R}_p^t, \qquad (11)$$

where the term in square brackets is equal to $\mathcal{R}_p^{t+1}$ from (9). Minimizing the long-term average of (11) minimizes the system churn rate. The total cost incurred in time slot t is defined as the sum of costs incurred by each program stream: i.e.,

$$c^t(s^t, a^t) = \sum_{p=1}^{\mathcal{P}_k} c_p^t(s_p^t, a_p^t), \qquad (12)$$

where $s^t = \{s_i^t \ldots s_{\mathcal{P}_k}\}$ and $a^t = \{a_i^t \ldots a_{\mathcal{P}_k}\}$ are joint state and actions, respectively.

The value of each state when following the policy Π is defined using *Value function*, $V^\Pi(s)$, given as:

$$V^\Pi(s) = \mathbb{E}\left[\sum_{t=0}^{\infty} (\omega)^t c^t(s^t, \Pi(s^t))|s = s^0\right], \qquad (13)$$

where $\omega \in [0, 1]$; $(\omega)^t$ is the t-th power of the discount factor. We take the expectation over a sequence of states that is governed by the controlled Markov chain with transition probabilities $P(s'|s, a) = \prod_{p=1}^{\mathcal{P}_k} P^{\mathcal{R}}(\mathcal{R}_p'|\mathcal{R}_p, a_p) \prod_{\tau=1}^{T_p} P^\gamma(\gamma_{p,\tau}'|\gamma_{p,\tau})$. We can represent expected future cost using the recursive expression of the value function based on the transition probability as: $V^\Pi(s) = c(s, \Pi(s)) + \omega \sum_{s'\in S} P(s'|s, \Pi(s))V^\Pi(s')$.

Then, the objective of the resource allocation strategy is to determine the resource allocation and tile encoding policy that solves the following optimization:

$$\min_{\Pi\in\boldsymbol{\Pi}} V^\Pi(s), \qquad (14)$$

where $\boldsymbol{\Pi}$ is the set of all the possible policies. The optimal solution to (14) satisfies the Bellman equation, $\forall s \in S$:

$$V^*(s) = \min_{a\in A} \left\{c(s, a) + \omega \sum_{s'\in S} P(s'|s, a)V^*(s')\right\}, \quad (15)$$

$$\triangleq \min_{a\in A} \psi^*(s, a), \qquad (16)$$

where $V^*(s)$ is the optimal value function. $\psi^*(s, a)$ is the optimal action-value function that evaluates the value of taking an action a in state s and thereafter following the optimal policy. The optimal policy $\Pi^*(s)$ can be determined by taking the action that minimizes the right-hand side of (16) and thereby gives us the optimal action to take in each state.

Since the possibilities for quantization parameter selection and resource allocation are nearly infinite, there is a large number of discrete states and actions. Furthermore, the dynamics of the underlying system (user channel quality, user requests, video data rate adaptation, gNB radio resource allocation) is predominant and the complexity would be very high if the broadcast resource and encoding parameter allocation problem has to be entirely solved for each video GOP from scratch. For a scenario with P_k programs and $\mathcal{M}$ RBs, and each 360° program stream has T_p tiles and there are $|q| = q_{max} - q_{min}$ possible program stream data values and M possible MCS levels that can be allocated to the tiles of each program, then there are a total of $P_k \times \mathcal{M} \times T_p \times |q| \times M$ possible states and $\mathcal{M} \times M \times |q|$ possible resource allocation actions. Hence, we use DRL to solve this problem.

We use a deep neural network deterministic policy gradient method, DDPG algorithm. It is suitable for high dimensional, continuous or discrete, large action state space problems. The underlying principle is Actor-Critic framework consisting of an actor and a critic function. The former chooses the actions and latter evaluates the corresponding selection.

We employ DRL-based DDPG method that reduces the time complexity by maintaining a cache (i.e., replay buffer) with state-action transitions and by performing an iterative update of the networks (critic, actor, and target) on-the-go instead of exploring the state-action mapping each time from the beginning. The current policy is specified by mapping states to an action in the DNN (parameters η^μ) by means of an actor function, $\mu(s|\eta^\mu)$. The critic function, $\psi(s, a|\eta^\psi)$, is implemented using DNN (parameter: η^ψ) that learns using Bellman equation and provides feedback based on selected action. We update the actor DNN using gradient of the expectation of return J in terms of η^μ, similar to (13).

$$\nabla_{\eta^\mu} J \approx \mathbb{E}_{s^t \sim \rho^\delta}[\nabla_{\eta^\mu} \psi(s, a|\eta^\psi)|_{s=s^t, a=\mu(s^t|\eta^\mu)}]. \quad (17)$$

We update the critic network by minimizing the MSE:

$$L(\eta^\psi) = \mathbb{E}_{s^t \sim \rho^\delta, a^t \sim \delta, c^t \sim E}\left[(\psi(s^t, a^t|\eta^\psi) - y^t)^2\right], \quad (18)$$

$$y^t = c(s^t, a^t) + \omega\psi(s^{t+1}, \mu(s^{t+1})|\eta^\psi), \quad (19)$$

where, E is the stochastic environment that has been modeled as MDP, δ is the stochastic behavior policy, ρ denotes the discounted state visitation distribution, and y^t is the target value.

DDPG architectural modifications consisting of DNN function approximations are used to learn in large state-action spaces. The transition tuples (s^t, a^t, c^t, s^{t+1}) are stored in a replay buffer (finite-size cache) to prevent sample correlation. We update the actor-critic in each time step by sampling the stored transitions in the replay buffer, thereby learning from uncorrelated transitions. The divergence and stability due to the update in network and y^t using the same Q-network is addressed by considering copies and slow updates in these copies of the actor-critic networks. We add samples from a noisy process to the actor policy, $\mu'(s^t) = \mu(s^t|\psi_t^\mu) + \mathcal{N}$, where $\mathcal{N}$ is environment specific.

The storing of transition tuples in the replay buffer also enables an instantaneous update in action based on system state, preventing action computation each time. This reduces the time complexity to $\mathcal{O}(1)$ [31] by mapping the system state to an action from the cache that stores the $P_k \times \mathcal{M} \times T_p \times |q| \times M$ states. The agent in DRL-based method can instantly determine the action given the dynamic system information (user requests, SINR, channel characteristics, MBSFN group) while populating the replay memory cache on-the-go and simultaneously updating the deep neural network representing the action policy. Overall, the state, action, and networks (critic, actor, and target) are initialized (i.e. Steps 4 and 5 in Algorithm I-Function II) only once at the beginning. Thereafter, the long term cost (given by (11), Step 6 in Algorithm I-Function II)) is minimized by executing it each time the system state gets updated.

I2MB selects the efficient 360° video encoding parameters (quantization level $q_{p,\tau}^k$, $1 \leq \tau \leq T_p$) and performs optimal radio resource allocation for each program p in $\mathcal{P}$ and MBSFN k ($1 \leq k \leq K$). We formulate two dual objectives:

(i) I2MB($\mathcal{D}_{\min}$) minimizes the immersive multimedia broadcast service distortion for the served users in the system, and (ii) I2MB($\mathcal{Cr}_{\min}$) minimizes the churn rate, i.e. maximizes the number of served users N in the system with a guaranteed minimum acceptable video quality, subject to multiple system constraints. Particularly, the following needs to be ensured:

(a) the gNB capacity provides the upper bound to the total rate that can be broadcast to the heterogeneous UEs;

(b) the sum of proportional time-frequency resource block allocation to broadcast the various 360° immersive video content is upper bound to 1 at each gNB;

(c) all gNB in an MBSFN area need to use the same quantization level q_τ^p for tiles of program p, allocate the same set of radio resource σ_τ^p to each video tile τ, $1 \leq \tau \leq T_p$, and use the same MCS m_τ^p to broadcast it;

(d) the MCS selected to broadcast the immersive video tiles can belong to the set of allowed MCS levels in accordance with the 3GPP standard.

We formulate the respective optimization problems below, where the constraints (20a)-(20d) capture the above conditions.

$$I2MB(\mathcal{D}_{min}) : \min_{[q^1,...,q^K]} \sum_{i=1}^N \mathcal{D}_i, \quad (20)$$

$$\text{s.t.:} \quad \sum_{p=1}^{|\mathcal{P}|} \sum_{\tau=1}^{T_p} \mathbf{1}_{p,j} R(q_\tau^p)$$

$$\leq \sum_{p=1}^{|\mathcal{P}|} \sum_{\tau=1}^{T_p} \mathbf{1}_{p,j} C(\sigma_\tau^p, m_\tau^p), \quad (20a)$$

$$\sum_{p=1}^{|\mathcal{P}|} \sum_{\tau=1}^{T_p} \mathbf{1}_{p,j} \sigma_\tau^p \leq 1, \ \forall \text{gNB } j,$$
$$(20b)$$

$$q_{p,\tau}^k = q_\tau^p; \ \sigma_{p,\tau}^k = \sigma_\tau^p; \ m_{p,\tau}^k = m_\tau^p,$$
$$(20c)$$

$$\forall \tau, \ p \text{ broadcast in } k,$$

$$1 \leq m_{p,\tau}^k \leq 15, \forall \tau, k. \quad (20d)$$

$$I2MB(\mathcal{Cr}_{min}) : \min_{[q^1,...,q^K]} \mathcal{Cr}$$

$$\text{s.t.: } (20a) - (20d), \quad (21)$$

where the indicator function $\mathbf{1}_{p,j} = 1$ if gNB j broadcasts the program p. The vector of quantization levels used for encoding the tiles of video programs being broadcasted in MBSFN k ($p \in \mathcal{P}_k$, $1 \leq k \leq K$) is denoted as $q^k = [q_{1,1}^k, \ldots, q_{1,T_1}^k, \ldots, q_{P_k,1}^k, \ldots, q_{P_k,T_{P_k}}^k]$.

If gNB j is a part of MBSFN k and $p \in \mathcal{P}_k$ then it broadcasts p, provided atleast one or more users experience acceptable program quality $\mathcal{Q}_i > 0$. Thus, constraints (20c) and (20d) is subject to broadcast of program p by gNB j. Additionally, since gNB can belong to more than one MBSFN area, (20b)-(20c) applies to each gNB instead of an MBSFN area. Given program p and its tile τ, q_τ^p, σ_τ^p and m_τ^p appearing

---

Algorithm 1: I2MB: MBSFN Formation, Tile Encoding, and Resource Allocation

---

Input: u_i, $1 \leq i \leq N$, K

Function I: MBSFN_Formation (u_i, K):

1) **Select centroids from** u_i: c_1 randomly, c_k, $2 \leq k \leq K$,
    2) based on clustering policy.
2) **K-cluster formation:** Assign user i to cluster $k^\star$,
    $k^\star = \min_k d^2(u_i, c_k)$
3) **Cluster update:** Reassign centroid c_k to decrease
    1) average measure: $\left(\sum_{i=1}^{N} d^2(u_i, c_k) \right) / N$
4) Reiterate step 2-3 until cluster assignments
    1) are unchanged
5) gNB with UEs in cluster k, belongs to MBSFN area k
6) TV programs set broadcast in MBSFN k, $\mathcal{P}_k$, are those requested by users in cluster k

   return K MBSFN areas, $\{\mathcal{P}_k\}_k$

Function II: Resource_alloc_Tile_encoding_DDPG $(\{\mathcal{P}_k\}_k, u_i, i \in cluster\ k)$:

1) **Proportion of resource allocation to program tiles**
    for each program $p \in \mathcal{P}_k$
       for each tile $\tau = 1$ to T_p
          #users in k: N_k, #requesting τ of p: n_τ^p
          $\sigma_\tau^p = \frac{n_\tau^p}{N_k}$
2) **MCS allocation to program tiles**
    for each program $p \in \mathcal{P}_k$
       for each tile $\tau = 1$ to T_p
          $I2MB(\mathcal{D}_{min})$: $\overline{\gamma}$=least SINR, user subset
          $I2MB(\mathcal{C}_{min})$: $\overline{\gamma}$=least SINR, all users set
          Select $m_\tau^p = \min_m(SINR_{thr}(m) \geq \overline{\gamma})$
3) **Quantization parameter selection for video tiles**
    for each program $p \in \mathcal{P}_k$
       for each tile $\tau = 1$ to T_p
          Select $q_\tau^p = \max_q(C(\sigma_\tau^p, m_\tau^p) \geq R(q))$
          $\mathcal{R}_p = R(q)$
4) State $s^1 = \{\mathcal{R}_p, \gamma\}$ and action $a^1 = \{m_\tau^p, \sigma_\tau^p, q_\tau^p\}$
5) Initialize critic (ψ), actor (μ) and target (ψ', μ')
    1) networks
6) Minimize the long-term average of (11):
    for iteration= 1, $\mathcal{I}$ **do**
       Initialize random process $\mathcal{N}$ for action exploration
       for $t = 1, T$ **do**
          Select action $a^t = \mu(s^t | \eta^\mu) + \mathcal{N}^t$
          Execute a^t, observe c^t and s^{t+1}
          Store transition (s^t, a^t, c^t, s^{t+1}) in replay buffer
          Sample transitions (replay buffer): (s^i, a^i, c^i, s^{i+1})
          Set y^i using $c^i, s^{i+1}, \psi', \mu'$ in (19)
          Update critic by minimizing the loss in (18)
          Update actor policy: sample-policy-gradient in (17)
          Update target network:
             $\eta^{\psi'} \leftarrow \varrho\eta^\psi + (1-\varrho)\eta^{\psi'}$
             $\eta^{\mu'} \leftarrow \varrho\eta^\mu + (1-\varrho)\eta^{\mu'}$
       end for
    end for
    return $m_\tau^p, \sigma_\tau^p, q_\tau^p$

Output: K MBSFN areas, $\{\mathcal{P}_k\}_k$, $m_\tau^p, \sigma_\tau^p, q_\tau^p$

---

in (3b), (3c) The data rate $R(q_\tau^p)$ required for transmission of tile τ of program p is set by the encoder. The DDPG based resource allocation (MCS and resource block) and efficient tile encoding in the proposed I2MB framework using Algorithm 1 Function II.

The optimization problem I2MB$(\mathcal{D}_{min})$ is solved based on the following proposition that enables formulating a low-complexity solution to the problem described below:

Proposition 1: The objective (20) *is a strictly increasing function of the quantization levels* $[q^1, \ldots, q^K]$.

Proof: It is evident from Fig. 5 that both quality and rate are strictly decreasing functions of quantization parameter q. The distortion is a strictly increasing function of q. Analytically, we model $R(q) = a \cdot e^{b \cdot q}$ and $D(q) = c \cdot e^{d \cdot q}$, and $Q(q) = 10 \cdot \log_{10}(\frac{l_{max}}{D(q)})$. It is shown in Fig. 5(a) that this video rate model for Tile 40 of a 360-degree video corresponds to $a = 57500$ and $b = -0.2$ with RMSE = 0.00097. The video distortion (Y-MSE) model is shown in Fig. 5(b) for Tile 40 and it corresponds to $c = 11.2$ and $b = -0.12$ with RMSE = 0.00852. The video quality (V-PSNR) model for Tile 40 is shown in Fig. 5(c) and it has RMSE=0.00361.

The non-negative weighted linear sum of strictly increasing functions is increasing [32], [33]. Hence, we prove that our objective function is strictly increasing with the quantization level value by proving it for generic $\mathcal{D}_i$. The first derivative of $\mathcal{D}_i$ with respect to q_p^k (i.e., the quantization level of the program requested by u_i in the MBSFN(s) to which the UE belongs) is of the form $c \cdot q$ ($c > 0$ and a constant). This is positive thus proving the assertion. □

The objective function (20) with constraints (20a)-(20d) selects the highest possible quantization parameter level for the group of users requesting tiles of a program such that the resource constraint in the network are met.

The optimization problem for I2MB$(\mathcal{C}_{min})$ is solved by selecting the lowest possible m_τ^p and the highest possible $q_{p,\tau}$ $\forall \tau, p$ such that $Q(q_{p,\tau}) \geq Q_{min}$. This ensures that the maximum number of users in the system have $\phi=1$ which is in accordance with objective (21).

V. PERFORMANCE EVALUATION

FIGURE 6. Panoramic snapshots of 360° video.

To assess the performance of our scheme, we have used 360° videos with diverse content types (for example: Office, City, Sports, Jungle, and Sunrise). Sample snapshots of three videos from the set that has bee used is shown in Fig. 6. They have 4K spatial resolution, 1800 frames, and 30fps frame rate. Each video is divided into M = 64 tiles (8 × 8 tiling) that are compressed using HEVC [34] into 9 quality versions corresponding to 9 QP values of 16, 20, 24, 28, 32, 36, 40, 44, and 48. We use the 5G NR frequency range 1 (FR1) [5] network scenario for performance evaluation. The overall simulation parameters are listed in Table 1.

TABLE 1. Simulation parameters.

Parameter	Value
#epochs	50-100
learning rate	10^{-3}
Update parameter, ϱ	0.001
#hidden units (LSTM)	50
#hidden layers (DNN)	2
#neurons	300-400
Update rule	Adam
Steps per epoch	10000
Tests per epoch	10
Steps per test	2000
Batch size	16, 32
Replay memory size	1000 kB
Channel bandwidth	50 MHz
Frequency	3.4 GHz
Number of data carriers	1200
Receiver noise figure	7 dB
Maximum transmitter output power	46 dBm
Transmitter (Receiver) antenna gain	18 (0) dBi
Building loss	14.0 dB
Receiver sensitivity	-106.4 dBm
Shadowing standard deviation	8 dB
Average cell radius	720 m

A. HEAD NAVIGATION PREDICTION: LSTM FORECASTING

We have used the dataset [35] that is an aggregation of six different previously published datasets [36], [37], [38], [39], [40], [41]. The original datasets contained user head orientations while viewing 360 degree videos using a head mounted streaming device. This data is extracted, and preprocessed to yield a common representation. This dataset contains user head orientation trajectories for 3791 independent viewings of 88 different 360° videos with an average of 45 viewings per video. The total viewing duration is 514215 seconds (142 hours 50 minutes 15 seconds).

Fig. 7 shows the LSTM forecasting output of predicted pitch and yaw angle for one of the users while watching one of the immersive video content. Fig. 7(a) and (d) shows that the relative length of training sequence is less than 30% of the entire video duration, denoted as 'Observed'. Fig. 7(b) and (e) show that the predicted pitch and yaw angle values are very close to the observed user head navigation angles, respectively. The sample error (between the predicted and observed values) for the pitch and yaw angles is shown in Fig. 7(c) and (f), respectively, with an overall RMSE less than 0.1. This shows the efficacy of the LSTM forecasting model with network state update in predicting the head navigation direction of the heterogeneous users.

We studied the predictor performance for the entire set of 34 users viewing the 15 immersive video content. Fig. 8(a) shows the RMSE performance of the predictor for Pitch and Yaw angles when varying the relative training and predicted sample duration from less than 10% to 90% with 50 training epochs. It is observed that RMSE reduces with increase in relative training duration and also that RMSE of less than 0.01 is achieved with a 10 sec training duration. Fig. 8(b) shows the predictor RMSE when the maximum training epochs (iterations) are varied from 10 to 100. The RMSE reduces with
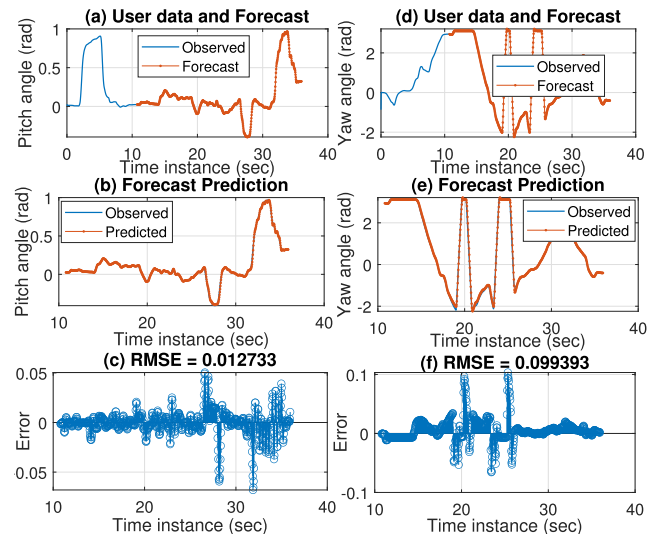

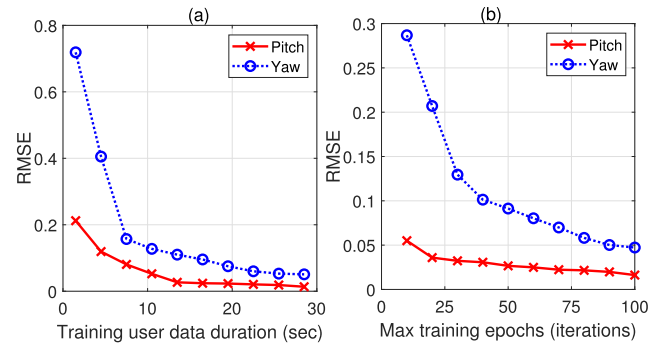**FIGURE 7.** Forecasting head navigation angles of users.

FIGURE 8. Head navigation angle prediction RMSE.

increase in the number of training iterations and RMSE of less than 0.01 is achieved with 30 or more iterations.

B. MBSFN AREA FORMATION: USER CLUSTERING

We have assessed K-means, K-medoids, and fuzzy c-means multi-criteria clustering algorithms to chose the most effective method to efficiently form the MBSFN areas. These clustering methods have been evaluated in terms of metrics listed in Section IV-B, i.e. Euclidean distance, Mahalanobis distance, Silhouette coefficient, and Dunn's index. The clustering performance of these methods in terms of the mentioned metrics is shown in Fig. 9(a)-(d), respectively. It is seen that K-means and K-medoid multi-criteria clustering methods have comparable and significantly better performance than fuzzy c-means in terms of the Euclidean and Mahalanobis distance. Furthermore, K-means efficacy as compared to K-medoid and Fuzzy c-means method is evident from its higher Dunn's index value, shown in Fig. f:cluster1(d).

The Silhouette value for the eight clusters formed in a scenario consisting of 70 users per cell and 10 programs using the three methods is shown in Fig. 10. Even though Fuzzy
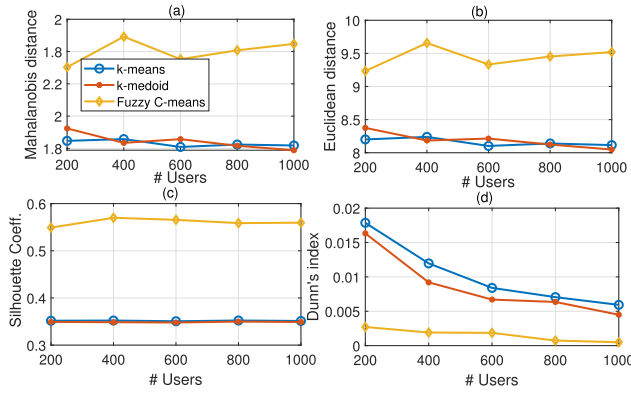
FIGURE 9. (a) Euclidean distance, (b) Mahalanobis distance, (c) Silhouette coefficient, (d) Dunn's index, for user clustering using k-means, k-medoid, and fuzzy c-means methods.
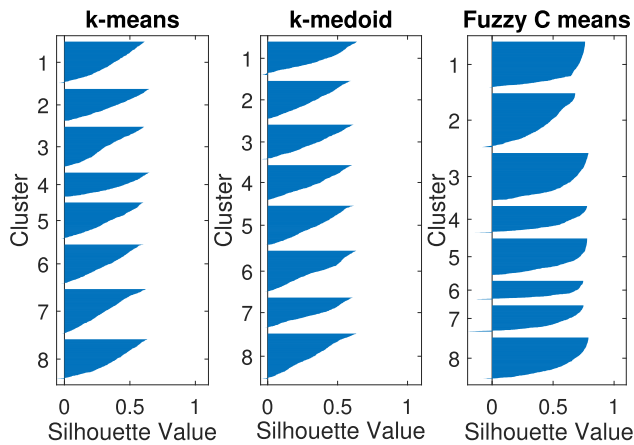

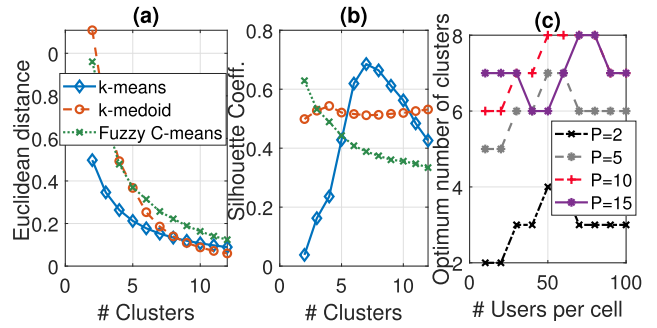**FIGURE 10.** Silhouette for user clustering using k-means, k-medoid, and fuzzy c-means methods.

FIGURE 11. (a) Euclidean distance and (b) Silhouette coefficient for increasing number of cluster. (c) Optimum number of clusters with increasing number of users per cell and broadcast program.
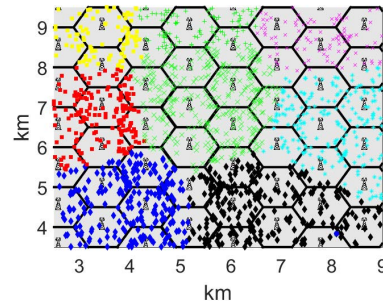

FIGURE 12. Multi-criteria K-means area formation (8 clusters).

c-means method has a higher Silhouette coefficient than the other two methods, as is evident from Fig. 9(c) and Fig. 10, we prefer K-means method due to its better performance in terms of other three metrics. Also, as can be seen from Fig. 10 the clusters are more balanced in terms of cluster size for K-means as compared to fuzzy c-means. This further motivates us to use K-means multi-criteria clustering method to form MBSFN areas in our I2MB framework.

Given a network scenario, we obtain the optimum number of clusters using the Euclidean and Silhouette method. According to the Elbow curve method [42] the optimal number of cluster is the point where Euclidean distance drops suddenly (*'Elbow'*).The optimal number of clusters maximizes the Silhouette coefficient [42]. It is again evident from Fig. 11(a) and 11(b) that K-means clustering can effectively use these methods to find the optimal number of clusters in a given scenario.

K-means multicriteria clustering implementation is a simple, easy, and effective method to classify data [43]. Additionally, it is fast with few computations and has linear complexity O(n). We therefore apply the Lloyds K-means heuristic [44] for our multi-criteria clustering of heterogeneous users into K MBSFN areas. The cluster centroids are selected using the

K-means++ approach [45]. The optimal number of clusters is system scenario dependent and can be assessed through Fig. 11(c). The optimum number of clusters depends on the number of users and number of programs. A few program options results in a fewer number of clusters (i.e. fewer MBSFN areas). As can be seen from Fig. 11(c), sometimes a higher number of users provides more competent centroid options resulting in lesser number of optimum clusters.

C. I2MB COMPARATIVE PERFORMANCE

Fig. 12 shows an instance of the network scenario we consider. It includes 200 uniformly randomly distributed users per cell and 52 gNodeB cells. Each user randomly views the broadcast program at a particular viewing angle based on the dataset [35]. The 5G NR simulation parameters are listed in Table 1. For each user in an MBSFN area with a given number of interfering cells, the SINR is computed according to [5]. The performance of our system is obtained by averaging the results over several iterations (>150 iterations with 95% confidence interval) with uniformly random distribution of users. We also examine the impact of the number of users.

Given the above scenario, our approach leads to the formation of an optimum number of MBSFN areas using the approach discussed in Section V-B. Eight clusters (MBSFN areas) are formed in the scenario shown in Fig. 12, indicated by different color markers. The efficacy of our proposed LSTM based viewport angle prediction scheme in I2MB is evident from the Fig. 13(a) that shows the viewport
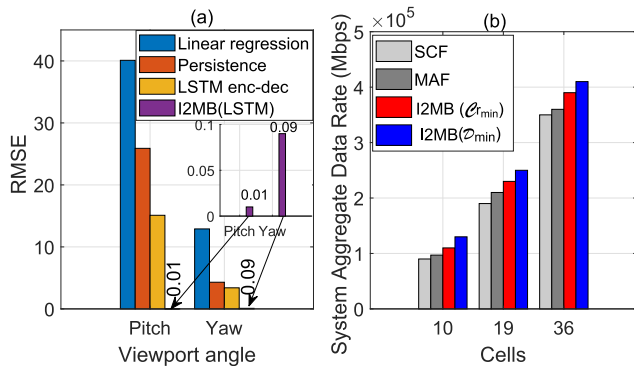
FIGURE 13. Performance comparison in terms of (a) RMSE and (b) System aggregate data rate.

yaw and pitch angle prediction RMSE with respect to linear regression, persistence, and LSTM enc-dec (encoder-decoder) schemes from the literature [46]. The linear regression uses a linear model, the persistence predictor uses the last known viewpoint, and LSTM enc-dec network predicts the mean viewpoint position every second [46]. Overall, it can be seen from Fig. 13(a) that the RMSE of our proposed viewport angle prediction scheme, I2MB(LSTM) is below 0.1 and this is significantly lower than the other schemes. The efficacy of the proposed LSTM based forecast scheme in I2MB is attributed to the network state update using the observed viewport angles instead of the predicted values, making the prediction model more efficient.

The efficacy of the proposed I2MB schemes in terms of MBSFN area formation and resource allocation is evaluated in terms of system aggregate data rate performance, shown in Fig. 13(b), with respect to Single Content Fusion (SCF) and MBSFN Area Formation (MAF) schemes [47] from literature. SCF comprises of interest similarity based overlapping MBSFN formation and MAF focuses on improving system aggregate data rate for video-on-demand requests by dynamically creating MBSFN Areas [47]. The proposed I2MB scheme benefits from dynamic MBSFN area formation, efficient resource allocation, and intelligent immersive multimedia encoding. Overall, it can be seen from Fig. 13(b) that I2MB ($\mathcal{C}r_{min}$) and I2MB ($\mathcal{D}_{min}$) schemes have a higher system aggregate data rate (on average) by 18.44%, 9.45% and 25.4%, 15.87% than SCF, MAF, respectively.

The significance of tile based immersive video broadcast in I2MB is evident from Fig. 14. Fig. 14(a) shows the total number of users requiring specific tile numbers of program $p = 1$ based on their viewing angles. It can be seen that there are some tiles (tiles 11-12, 29-30), based on heterogeneous users' viewing direction, that are being viewed by more users while a few others (tiles 16-18, 24-26) are not being viewed at all. The MCS selection for adaptive tile encoding based on the resource constraint and user distribution within a MBSFN area for these programs is shown in Fig. 14(b). Fig. 14(c) shows the corresponding efficient QP level, respectively. The corresponding quality in terms of viewport luminance PSNR (Y-PSNR) is shown in Fig. 14(d). The tile specific rates of
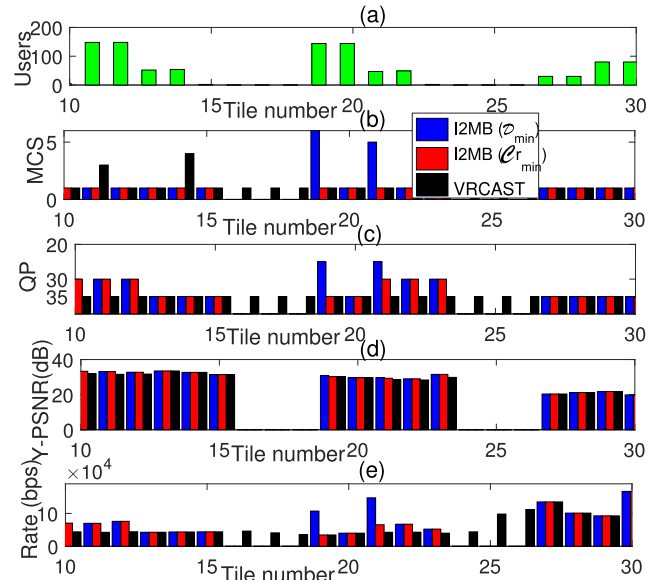

FIGURE 14. (a) Number of users requesting tiles (based on viewport), (b) MCS, (c) QP, (d) Quality (Y-PSNR in dB), and (e) Rate for tiles of Program $p = 1$.
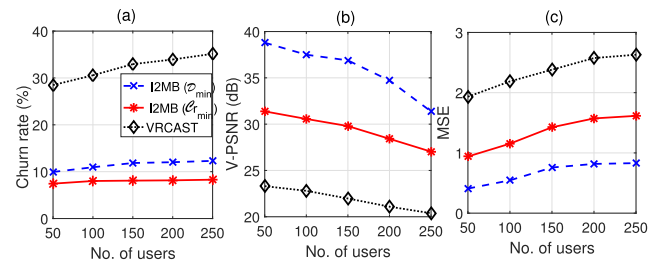

FIGURE 15. (a) Churn rate, (b) Viewport PSNR, and (c) MSE for I2MB with increasing number of users per cell.
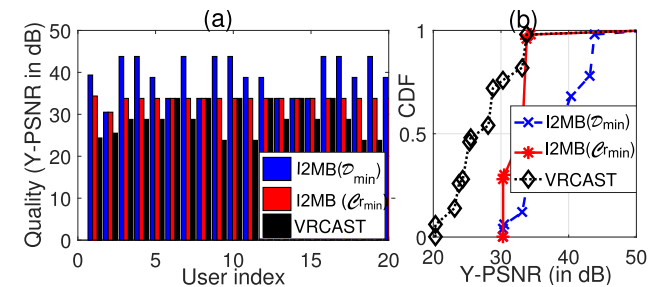

FIGURE 16. (a) Quality (Y-PSNR in dB), (b) CDF of Quality.

the tiles of this program is shown in Fig. 14(e). I2MB (both $\mathcal{D}_{min}$ and $\mathcal{C}r_{min}$ schemes) selects efficient QP and MCS level as compared to existing scheme (VRCAST [12]) in dense network scenario while ensuring higher tile quality delivered to users.

We also examine the performance of I2MB (both $\mathcal{D}_{min}$ and $\mathcal{C}r_{min}$ schemes) in terms of the churn rate (i.e., proportion of unserved users), immersive video quality (in terms of viewport PSNR) and distortion (MSE). It is evident from Fig. 15(a) that the churn rate increases as the number of users per cell increases. The churn rate of I2MB($\mathcal{D}_{min}$) and I2MB($\mathcal{C}r_{min}$)

is 65.63% and 71.88% (on average) lower than VRCAST. The Viewport PSNR (V-PSNR) reduces with an increase in number of users per cell but is maintained above 27 dB for the two I2MB methods unlike VRCAST that has 23 dB V-PSNR, as shown in Fig. 15(b). The MSE increases with increase in number of users and the performance of I2MB($\mathcal{D}_{min}$) and I2MB($\mathcal{Cr}_{min}$) is 76.14% and 42.28% better (i.e. lower distortion, MSE), respectively, than the existing scheme [12], as shown in Fig. 15(c).

The quality per user for a scenario with fifty users in each cell is shown in Fig. 16(a) and the corresponding cumulative distribution function (CDF) is shown in Fig. 16(b). It is evident from Fig. 16 that I2MB($\mathcal{D}_{min}$) and I2MB($\mathcal{Cr}_{min}$) provides higher quality (greater than 30dB) for all users as compared to VRCAST. Specifically, as can be seen from Fig. 16(a), for example, user 1, 3, and 4 receive Y-PSNR greater than 40 dB using I2MB($\mathcal{D}_{min}$) and $\approx$35 dB using I2MB($\mathcal{Cr}_{min}$), while VRCAST provides <30dB Y-PSNR in the given dense urban network scenario. The CDF in Fig. 16(b) shows the I2MB in guaranteeing a higher video quality to the heterogeneous users.

VI. CONCLUSION

We have developed a novel and efficient intelligent immersive multimedia broadcast scheme, I2MB, for next generation cellular networks, that significantly improves the overall 360° video quality while serving an increased number of heterogeneous users. It considers the users' channel conditions, viewing angle, and service requests for adaptively broadcasting the 360° immersive video content. The time series forecasting of head navigation direction of users is performed using LSTM deep learning model. Thereafter, I2MB scheme performs the multi-criteria K-means clustering with optimal number of clusters to dynamically and efficiently define the MBSFN areas. We optimally encode immersive video tiles and perform efficient radio resources allocation using Deep Reinforcement Learning (DRL) Deep Deterministic Policy Gradient algorithm to either minimize the immersive broadcast video distortion (i.e. I2MB($\mathcal{D}_{min}$) scheme) or minimize the churn rate (i.e. I2MB($\mathcal{Cr}_{min}$) scheme). We have shown that our proposed framework, I2MB, outperforms other recent scheme by providing $\approx$ 14 and 8 dB improvement in quality while serving 28.47% and 37.14% higher number of heterogeneous users with $\mathcal{D}_{min}$ and $\mathcal{Cr}_{min}$ schemes, respectively, in a large-dense cellular network. This framework will further be extended to include complex scenarios with revenue models in next-generation cellular networks.

REFERENCES

[1] M. Hosseini and V. Swaminathan, "Adaptive 360 VR video streaming: Divide and conquer," in *Proc. IEEE Int. Symp. Multimedia (ISM)*, San Jose, CA, USA, Jan. 2016, pp. 107–110.

[2] M. Hosseini, "View-aware tile-based adaptations in 360 virtual reality video streaming," in *Proc. IEEE Virtual Reality (VR)*, Los Angeles, CA, USA, Mar. 2017, pp. 423–424.

[3] C. Singhal and S. De, "Energy-efficient and QoE-aware TV broadcast in next-generation heterogeneous networks," *IEEE Commun. Mag.*, vol. 54, no. 12, pp. 142–150, Dec. 2016.

[4] L. Richter, M. Hoyer, and S. Ilsen, "A software defined radio based FeMBMS measurement receiver: Test results," in *Proc. IEEE Int. Symp. Broadband Multimedia Syst. Broadcast. (BMSB)*, Jeju, South Korea, Jun. 2019, pp. 1–9.

[5] J. J. Gimenez, J. L. Carcel, M. Fuentes, E. Garro, S. Elliott, D. Vargas, C. Menzel, and D. Gomez-Barquero, "5G new radio for terrestrial broadcast: A forward-looking approach for NR-MBMS," *IEEE Trans. Broadcast.*, vol. 65, no. 2, pp. 356–368, Jun. 2019.

[6] M. Tavakoli and M. Cave, "Modelling television viewing patterns," *J. Advertising*, vol. 25, no. 4, pp. 71–86, Dec. 1996.

[7] A. J. B. Chaney, M. Gartrell, J. M. Hofman, J. Guiver, N. Koenigstein, P. Kohli, and U. Paquet, "A large-scale exploration of group viewing patterns," in *Proc. ACM Int. Conf. Interact. Experiences TV Online Video*, 2014, pp. 31–38.

[8] C. Chen, Y. Zhu, F. Tian, and R. Hu, "The study of viewing behaviors based on gazing points visualization," in *Proc. Int. Conf. Audio, Lang. Image Process. (ICALIP)*, Shanghai, China, Jul. 2018, pp. 35–40.

[9] X. Kui, H. Lv, Z. Tang, H. Zhou, W. Yang, J. Li, J. Guo, and J. Xia, "TVseer: A visual analytics system for television ratings," *Vis. Informat.*, vol. 4, no. 3, pp. 1–11, Sep. 2020.

[10] H. M. Moghaddam, G. Acar, B. Burgess, A. Mathur, D. Y. Huang, N. Feamster, E. W. Felten, P. Mittal, and A. Narayanan, "Watching you watch: The tracking ecosystem of over-the-top TV streaming devices," in *Proc. ACM SIGSAC Conf. Comput. Commun. Secur.*, London, U.K., Nov. 2019, pp. 131–147.

[11] A. Yaqoob and G.-M. Muntean, "A weighted tile-based approach for viewport adaptive 360° video streaming," in *Proc. IEEE Int. Symp. Broadband Multimedia Syst. Broadcast. (BMSB)*, Paris, France, Oct. 2020, pp. 1–7.

[12] O. Eltobgy, O. Arafa, and M. Hefeeda, "Mobile streaming of live 360-degree videos," *IEEE Trans. Multimedia*, vol. 22, no. 12, pp. 3139–3152, Dec. 2020.

[13] J. Chen, M. Chiang, J. Erman, G. Li, K. K. Ramakrishnan, and R. K. Sinha, "Fair and optimal resource allocation for LTE multicast (eMBMS): Group partitioning and dynamics," in *Proc. IEEE INFOCOM*, Hong Kong, Apr. 2015, pp. 1–6.

[14] A. de la Fuente Iglesias, R. P. Leal, and A. G. Armada, "Performance analysis of eMBMS in LTE: Dynamic MBSFN areas," in *Proc. OPNETWORK*, Washington, DC, USA, Aug. 2013, pp. 1–6.

[15] M. Dorraki, A. Fouladzadeh, S. J. Salamon, and A. Allison, "Can C-reactive protein (CRP) time series forecasting be achieved via deep learning?" *IEEE Access*, vol. 7, pp. 59311–59320, 2019.

[16] R. Chandra, S. Goyal, and R. Gupta, "Evaluation of deep learning models for multi-step ahead time series prediction," *IEEE Access*, vol. 9, pp. 83105–83123, 2021.

[17] B. Farsi, M. Amayri, N. Bouguila, and U. Eicker, "On short-term load forecasting using machine learning techniques and a novel parallel deep LSTM-CNN approach," *IEEE Access*, vol. 9, pp. 31191–31212, 2021.

[18] B. Picano, R. Fantacci, and Z. Han, "Nonlinear dynamic chaos theory framework for passenger demand forecasting in smart city," *IEEE Trans. Veh. Technol.*, vol. 68, no. 9, pp. 8533–8545, Sep. 2019.

[19] J. Villegas, E. Baena, S. Fortes, and R. Barco, "Social-aware forecasting for cellular networks metrics," *IEEE Commun. Lett.*, vol. 25, no. 6, pp. 1931–1934, Jun. 2021.

[20] Y. Zhao, X. Wang, R. Wang, Y. Yang, and F. Lv, "Path planning for mobile robots based on TPR-DDPG," in *Proc. Int. Joint Conf. Neural Netw. (IJCNN)*, Shenzhen, China, Jul. 2021, pp. 1–8.

[21] K. Yang, C. Shen, and T. Liu, "Deep reinforcement learning based wireless network optimization: A comparative study," in *Proc. IEEE Conf. Comput. Commun. Workshops (INFOCOM WKSHPS)*, Toronto, ON, Canada, Jul. 2020, pp. 1248–1253.

[22] Z. Yang, Y. Liu, and Y. Chen, "Q-learning for content placement in wireless cooperative caching," in *Proc. IEEE Global Commun. Conf. (GLOBECOM)*, Abu Dhabi, United Arab Emirates, Dec. 2018, pp. 1–6.

[23] F. Fu, Y. Kang, Z. Zhang, F. R. Yu, and T. Wu, "Soft actor–critic DRL for live transcoding and streaming in vehicular fog-computing-enabled IoV," *IEEE Internet Things J.*, vol. 8, no. 3, pp. 1308–1321, Feb. 2021.

[24] D. P. Kingma and J. Ba, "Adam: A method for stochastic optimization," 2014, *arXiv:1412.6980*.

[25] Z. Zhang, "Improved Adam optimizer for deep neural networks," in *Proc. IEEE/ACM 26th Int. Symp. Quality Service (IWQoS)*, Banff, AB, Canada, Jun. 2018, pp. 1–5.

[26] D. Aloise, A. Deshpande, P. Hansen, and P. Popat, "NP-hardness of Euclidean sum-of-squares clustering," *Mach. Learn.*, vol. 75, no. 2, pp. 245–248, 2009.

[27] N. K. Verma and A. Roy, "Self-optimal clustering technique using optimized threshold function," *IEEE Syst. J.*, vol. 8, no. 4, pp. 1213–1226, Dec. 2014.

[28] P. J. Rousseeuw, "Silhouettes: A graphical aid to the interpretation and validation of cluster analysis," *J. Comput. Appl. Math.*, vol. 20, no. 1, pp. 53–65, 1987.

[29] P. Agrawal, N. K. Verma, S. Agrawal, and S. Vasikarla, "Color segmentation using improved mountain clustering technique version-2," in *Proc. 8th Int. Conf. Inf. Technol., New Generat.*, Las Vegas, NV, USA, Apr. 2011, pp. 536–542.

[30] J. C. Dunn, "Well-separated clusters and optimal fuzzy partitions," *J. Cybern.*, vol. 4, no. 1, pp. 95–104, 2008.

[31] J. Lin, Y. Zout, X. Dong, S. Gong, D. T. Hoang, and D. Niyato, "Deep reinforcement learning for robust beamforming in IRS-assisted wireless communications," in *Proc. IEEE GLOBECOM*, Taiwan, pp. 1–6, Dec. 2020.

[32] A. Cambini and L. Martein, *Convexity and Optimization: Theory and Applications*. Berlin, Germany: Springer-Verlag, 2009.

[33] S. Boyd and L. Vandenberghe, *Convex Optimization*. New York, NY, USA: Cambridge Univ. Press, 2004.

[34] G. J. Sullivan, J.-R. Ohm, W.-J. Han, and T. Wiegand, "Overview of the high efficiency video coding (HEVC) standard," *IEEE Trans. Circuits Syst. Video Technol.*, vol. 22, no. 12, pp. 1649–1668, Dec. 2012.

[35] A. Dharmasiri, C. Kattadige, V. Zhang, and K. Thilakarathna, "Viewport-aware dynamic 360° video segment categorization," in *Proc. 31st ACM Workshop Netw. Operating Syst. Support Digit. Audio Video*, Jul. 2021, pp. 114–121.

[36] X. Corbillon, F. De Simone, and G. Simon, "360-degree video head movement dataset," in *Proc. 8th ACM Multimedia Syst. Conf.*, Jun. 2017, pp. 199–204.

[37] W.-C. Lo, C.-L. Fan, J. Lee, C.-Y. Huang, K.-T. Chen, and C.-H. Hsu, "360-degree video viewing dataset in head-mounted virtual reality," in *Proc. ACM Multimedia Syst. Conf.*, Jun. 2017, pp. 211–216.

[38] Y. Bao, H. Wu, T. Zhang, A. A. Ramli, and X. Liu, "Shooting a moving target: Motion-prediction-based transmission for 360-degree videos," in *Proc. IEEE Int. Conf. Big Data*, Washington, DC, USA, Dec. 2016, pp. 1161–1170.

[39] C. Wu, Z. Tan, Z. Wang, and S. Yang, "A dataset for exploring user behaviors in VR spherical video streaming," in *Proc. 8th ACM Multimedia Syst. Conf.*, Jun. 2017, pp. 193–198.

[40] Y. Guan, C. Zheng, X. Zhang, Z. Guo, and J. Jiang, "Pano: Optimizing 360° video streaming with a better understanding of quality perception," in *Proc. ACM Special Interest Group Data Commun.*, Aug. 2019, pp. 394–407.

[41] A. T. Nasrabadi, A. Samiei, A. Mahzari, R. P. Mcmahan, R. Prakash, M. C. Q. Farias, and M. M. Carvalho, "A taxonomy and dataset for 360° videos," in *Proc. 10th ACM Multimedia Syst. Conf.*, Jun. 2019, pp. 273–278.

[42] T. Li, G. Kou, Y. Peng, and P. S. Yu, "An integrated cluster detection, optimization, and interpretation approach for financial data," *IEEE Trans. Cybern.*, early access, Sep. 22, 2021, doi: 10.1109/TCYB.2021.3109066.

[43] G. A. Wilkin and X. Huang, "A practical comparison of two K-means clustering algorithms," *BMC Bioinf.*, vol. 9, no. S6, pp. 1–5, May 2008.

[44] L. Galluccio, O. Michel, and P. Comon, "Unsupervised clustering on multi-component datasets: Applications on images and astrophysics data," in *Proc. Eur. Signal Process. Conf.*, Lausanne, Switzerland, Apr. 2008, pp. 1–5.

[45] D. Arthur and S. Vassilvitskii, "k-means++: The advantages of careful seeding," in *Proc. ACM SIAM*, Philadelphia, PA, USA, Jan. 2007, pp. 1027–1035.

[46] M. Jamali, S. Coulombe, A. Vakili, and C. Vazquez, "LSTM-based viewpoint prediction for multi-quality tiled video coding in virtual reality streaming," in *Proc. IEEE Int. Symp. Circuits Syst. (ISCAS)*, Seville, Spain, Oct. 2020, pp. 1–5.

[47] F. Rinaldi, S. Pizzi, A. Orsino, A. Iera, A. Molinaro, and G. Araniti, "A novel approach for MBSFN area formation aided by D2D communications for eMBB service delivery in 5G NR systems," *IEEE Trans. Veh. Technol.*, vol. 69, no. 2, pp. 2058–2070, Feb. 2020.

CHETNA SINGHAL (Senior Member, IEEE) received the B.Eng. degree in electronics and telecommunications from the University of Pune, India, in 2008, and the M.Tech. degree in computer technology and the Ph.D. degree from the Indian Institute of Technology (IIT) Delhi, in 2010 and 2015, respectively. She worked at the IBM Software Laboratory, New Delhi, as a Software Engineer, in 2010. She has been an Assistant Professor with the Department of Electronics and Electrical Communication Engineering, IIT Kharagpur, since 2015. She is currently a Visiting Researcher (an ERCIM Fellow) with the Department of Computer Science, RISE Research Institutes of Sweden. Her research interests include next generation heterogeneous wireless networks, with emphasis on cross-layer optimization, adaptive multimedia services, energy efficiency, and resource allocation.

• • •